

Aircraft Measurements of Convective Draft Cores in MONEX

CHARLES WARNER AND DONNA P. MCNAMARA¹

Department of Environmental Sciences, University of Virginia, Charlottesville, VA 22903

(Manuscript received 11 July 1983, in final form 5 October 1983)

ABSTRACT

Refinements have been made to a standard procedure for calculating vertical air velocities from parameters measured routinely during flights by the Electra aircraft of the National Center for Atmospheric Research. Accuracies generally near one or two meters per second have been attained.

Using this procedure with the Electra aircraft, together with data from one of the WP-3D aircraft of the National Oceanic and Atmospheric Administration, a survey has been made of 99 different updraft cores and 43 downdraft cores encountered during the Winter and Summer Monsoon Experiments, in which vertical air speed exceeded 2 m s^{-1} for 1 s. Ignoring peripheral drafts of speed less than the threshold 1 m s^{-1} , MONEX updraft cores were of median width 1.4 km, median peak updraft 3.2 m s^{-1} , mean updraft 2.3 m s^{-1} and \log_{10} (mass transport, in $\text{kg s}^{-1} \text{ m}^{-1}$ normal to the flight track) equal to 3.4. Downdraft cores were of median width 1.3 km, peak downdraft 2.6 m s^{-1} , mean downdraft 1.9 m s^{-1} and \log (mass transport) equal to 3.2. The greatest 1 s updrafts reached 17 m s^{-1} .

For draft cores other than in vigorous cumulonimbus, an equation was found relating mean draft speed, air density and width. Generally the mean draft speed approximately equals 2.5 m s^{-1} .

Characteristics of draft cores were found to be similar to those found over the tropical Atlantic by LeMone and Zipser.

1. Introduction

The purpose of this paper is to present a survey of updraft and downdraft cores encountered by U.S. research aircraft during the Winter and Summer Monsoon Experiments. The field phase of WMONEX has been described by Greenfield and Krishnamurti (1979), that of SMONEX by Fein and Kuettner (1980). Vertical air velocities averaged over 1 s of flight ($\sim 150 \text{ m}$) were computed. LeMone and Zipser (1980, hereafter referred to as LZ) and Zipser and LeMone (1980) have studied observations of this nature made in the GARP Atlantic Tropical Experiment (GATE), and elsewhere. Their data included 10^4 km of flight legs flown on 6 days in GATE. The results reported in this extension of their work come from 10^5 km of flight, mostly in the middle troposphere, on 16 days.

2. Data

The WP-3D aircraft of the National Oceanic and Atmospheric Administration flew six missions treated here over the South China Sea, and five missions treated here during summer MONEX. The Electra L-188 aircraft of the National Center for Atmospheric Research (NCAR) flew, respectively, five and eight such missions. The dates are given in Table 1. In this account

missions will be abbreviated as follows: "P10" will refer to the WP-3D on 10 December 1978, for instance, while for summer MONEX, over the Arabian Sea in June and the Bay of Bengal in July, the month will be included: for instance "E624" will refer to the Electra on 24 June 1979. (Abbreviations are included in Table 1.)

Aboard the WP-3D, measurements were made at 40 Hz and vertical air velocities were computed as a series of 1 s average values (Merceret and Davis, 1981). The nominal uncertainty in vertical drafts was 0.5 m s^{-1} . Vertical velocity traces were compared with side-camera films and/or Warner's photographs or flight log. It was found that calculated vertical air velocities were generally near zero during flight in clear air. Systematic departures from zero, in clear air, of $\sim -0.3 \text{ m s}^{-1}$ on mission P705, and $+0.3 \text{ m s}^{-1}$ on missions P707 and P708 were detected by visual inspection of time-series plots, and corresponding small corrections were applied uniformly to all data from these three missions. During WMONEX the ambient level of fluctuation in the WP-3D records was relatively great, generally about $\pm 0.7 \text{ m s}^{-1}$, and only cores of speed exceeding 5 m s^{-1} were examined, in studies of extremes.

Aboard the Electra, analog signals were recorded digitally at 50 Hz and averaged to yield mean 1 s values of measured parameters. The measurements have been described by Lenschow *et al.* (1978) and LeMone and Pennell (1980). Based on the technique of Kelly and

¹ Present affiliation: Det. 20, 17WS USAF, Little Rock AFB, Jacksonville, AR 72076.

TABLE 1. Dates of flights and numbers of draft cores recorded in each mission, from the WP-3D and the Electra. Numbers of updraft cores with $w_i = 1 \text{ m s}^{-1}$ are given, with downdrafts following in parentheses.

Date (and abbreviation)	Draft cores	
	(WP-3D)	(Electra)
9 December 1978 (9)	*6 (1)	
10 December 1978 (10)	*5 (0)	None
11 December 1978 (11)	*4 (0)	None
12 December 1978 (12)	*None	2 (1)
16 December 1978 (16)	*4 (0)	0 (2)
17 December 1978 (17)	*6 (0)	2 (4)
20 June 1979 (620)		**9 (6)
24 June 1979 (624)		8 (0)
3 July 1979 (703)	7 (1)	
5 July 1979 (705)	11 (1)	8 (0)
6 July 1979 (706)	7 (9)	
7 July 1979 (707)	**11 (1)	13 (1)
8 July 1979 (708)	0 (1)	13 (4)
14 July 1979 (714)		**2 (3)
18 July 1979 (718)		6 (3)
24 July 1979 (724)		0 (7)

* For the WP-3D in December, results are with $w_i = 5 \text{ m s}^{-1}$. Flights were generally in mid to lower troposphere.

** Indicates cores found at pressures $\geq 940 \text{ hPa}$ (in all, 7 updraft and 5 downdraft cores).

Lenschow (1978), calculations of vertical air velocity followed, as described in Appendix A. These calculations were checked using data from the gust probe aboard the Electra (Lenschow *et al.*, 1978), as described in Section 4.

Data on all cores were examined subjectively before inclusion in the survey. Some cores were excluded when other data were apparently incorrect. Aircraft attitude, thermodynamic and wind data, and photographs or observer notes were inspected for consistency with the presence of a core. Cores involving roll of the aircraft $> 10^\circ$ were excluded, unless the core appeared to have forced the roll.

Examination of the available data, generally cloud films made during the flights, indicated that all MONEX draft cores either were in cloud, or immediately adjacent to cloud, except during missions E620 and E714, during flight below cloud base. They generally occurred as groups of updraft cores in cumulus, or groups of downdraft cores in anvil cloud, without local balance of upward and downward mass fluxes in convective cores.

The survey may not be perfectly representative of the strong cores because some real cores may have been excluded during screening, and because the pilots—with safety in mind—sometimes avoided violent clouds.

3. Calculations on convective draft cores

LeMone and Zipser defined a “draft” as being continuously positive (or negative) for $\geq 500 \text{ m}$ and ex-

ceeding 0.5 m s^{-1} in magnitude for $\geq 1 \text{ s}$. They defined a “core” as exceeding 1 m s^{-1} for $\geq 500 \text{ m}$. To limit the scope of this study, and because of uncertainties in small derived values of vertical velocities, only “cores” are considered here, defined as exceeding 2 m s^{-1} for $\geq 1 \text{ s}$. The boundaries of cores were defined in terms of a threshold vertical velocity, w_i , generally 1 m s^{-1} . (A core of duration $\geq 500 \text{ m}$ with $w_i = 1 \text{ m s}^{-1}$ would be equivalent to one of LZ’s cores.) Statistics for $w_i = 1, 2, 3, 4$ and 5 m s^{-1} were explored, with a view to extrapolation to $w_i = 0$ (as opposed to relying on measurements of small vertical air velocities). A core with $w_i = 1 \text{ m s}^{-1}$ often involved several cores defined using a greater value of w_i .

Vertical velocities in cores were abstracted as a series of values every second, beginning from that second preceding the increase of speed through a threshold w_i , and ending at that second following the decrease of speed through the threshold w_i . Pressure, temperature, dew point and true airspeed (U) were noted for each core. Care was taken to avoid problems of sensor wetting in cloud by following the procedure described in Zipser *et al.* (1981, p. 1729); then density (ρ) was calculated.

Let the series of values of core strength (w) take the series of subscripts 1 to n ($n \geq 3$), as indicated in Fig. 1. The duration (T , s) of the core was taken as

$$T = f_1 + (n - 3) + f_2, \quad (1)$$

where the fractions of one second

$$\left. \begin{aligned} f_1 &= \frac{w_2 \mp w_i}{w_2 - w_i} \\ f_2 &= \frac{w_{n-1} \mp w_i}{w_{n-1} - w_n} \end{aligned} \right\} \quad (2)$$

The \mp signs refer to updraft or downdraft cores, respectively. The total mass flux (F) in the core was evaluated for a unit strip of width one meter across the flight track (LZ, p. 2448). In the units $\text{kg s}^{-1} \text{ m}^{-1}$,

$$F = 0.5\rho U [f_1(w_2 \pm w_i) + f_2(w_{n-1} \pm w_i) + (w_2 + w_{n-1}) + \sum_{i=3}^{n-2} 2w_i], \quad (3)$$

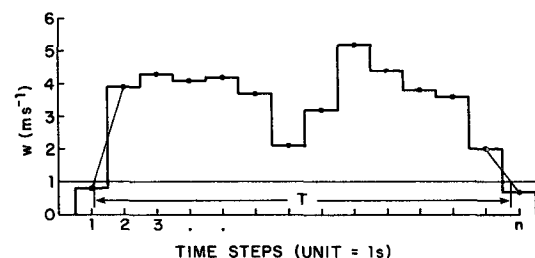


FIG. 1. Vertical velocity as a function of time in a typical core of duration T seconds given by Eq. (1), with the threshold $w_i = 1 \text{ m s}^{-1}$.

the \pm signs referring to updrafts and downdrafts respectively, the third term applying only when $n \geq 4$ and the last term only when $n \geq 5$.

The width of the core was taken as

$$d = UT. \tag{4}$$

This measure was called the diameter by LZ.

The mean speed of the core was taken as

$$\bar{w} = \frac{F}{\rho d}. \tag{5}$$

4. Comparison between (a) gust probe data and (b) computed vertical air velocities

In this section the computation of vertical air velocity (called method b), used in this work for the Electra aircraft, is compared with results from the Electra gust probe (method a). R. B. Friesen of NCAR has provided preliminary gust probe data (personal communication, October 1982) from the Electra, as a series of 1 s values of vertical air velocity measured on missions E620 and E624. These are to be compared with calculations (b) as described in Appendix A. Time series of results by methods (a) and (b) are shown in Fig. 2. Mass fluxes computed by methods (a) and (b) are plotted together in Fig. 3. Results by method (b) follow those by method (a) well. Fig. 3 indicates slight underestimation by method (b) of mass fluxes on 24 June, but 90% of the fluxes calculated by method (b) fall within 1.5 dB of the central 45° line.

It is important to note that there were many cores obtained by method (a) and not by (b). These are plotted along the abscissa in Fig. 3. These are cores encountered during climb, descent, or at roll $> 10^\circ$, when method (b) was not considered reliable.

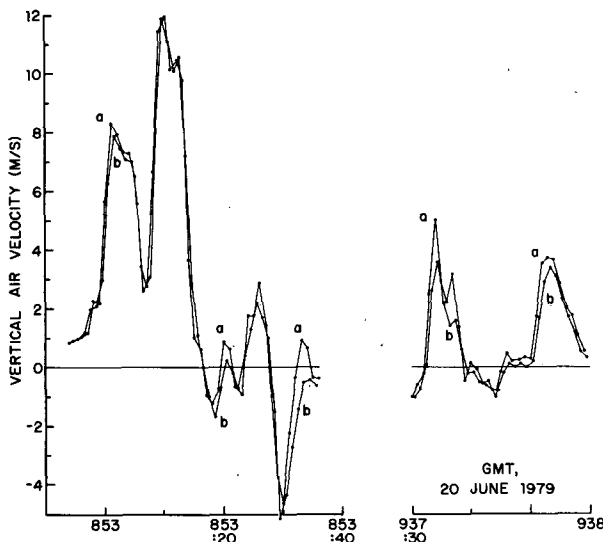


FIG. 2. Time series of vertical air velocities calculated by methods (a) and (b) for cores found on mission E620.

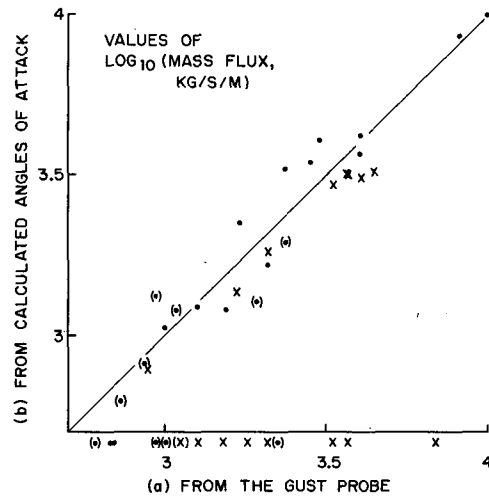


FIG. 3. Comparison of mass fluxes calculated by methods (a) and (b). Dots refer to mission E620 and crosses to E624. Downdraft cores are shown in parentheses. Many cores were obtained by method (a) and not by (b), during flight other than straight and level; these are plotted along the abscissa.

Method (b) differs from (a) in that results from (b), though evaluated every second, are nominally averages over 2 s; method (a) results are 1 s averages. In this work the series (b) are treated as 1 s averages. The agreement between methods (a) and (b) shown in Figs. 2 and 3 indicates that this procedure leads to no more than small error. The gust probe data are preliminary and may not be perfect (R. B. Friesen, personal communication). Discrepancies between the two sets of results may be attributed partly to uncertainties in method (a).

Kelly and Lenschow (1978) investigated measurements of vertical air velocities in inflow regions near cloud bases of thunderstorms, using an NCAR Queen Air (of wing area 27 m² as opposed to 121 m² for the Electra). They compared measurements using a gust probe (Lenschow *et al.*, 1978) with computations as described above. Differences in derived vertical air velocities were generally only tenths of meters per second (their Fig. 2). One draft of $\sim 16 \text{ m s}^{-1}$ yielded a difference between the two methods of 5 m s⁻¹. A similar case on 20 June 1979 yielded strikingly good agreement (Fig. 2 of this paper). It appears that method (b) yields results good mostly to a few tenths of meters per second for mean drafts, a few meters per second for peak drafts on the order of 10 m s⁻¹, and $\sim 1.5 \text{ dB}$ for the logarithm of mass fluxes, or a factor 1.4 in mass fluxes.

5. Frequency histograms of cores

Calculations as described in Section 3 were carried out for all the draft cores encountered during the missions shown in Table 1. Separate calculations were made for cases of the threshold w_t equaling 1, 2, 3, 4

and 5 m s^{-1} . In this section histograms are examined for $w_i = 1 \text{ m s}^{-1}$.

Histograms for widths (d) of cores are shown in Fig. 4; of peak vertical velocities w_p in Fig. 5a; of mean vertical velocities \bar{w} in Fig. 5b, and of mass fluxes in Fig. 6. These have been prepared in the same format as in LZ, and may be compared with the plots of cores at top left of pp. 2450–3 respectively of LZ, which apply over the altitude range 4.3 to 8.1 km. Most of the present data were gathered in the same altitude range; because dependences on altitude were slight (see Section 6 below), the present results were not stratified by altitude. Characteristics of the cores are presented in Table 2.

Results from the different regimes indicated in Figs. 4–6, over the South China Sea, Arabian Sea and Bay of Bengal, show no distinct differences. The evidence is consistent with a similarity of characteristics of convective draft cores in each area. Despite differences in approach, the MONEX results are generally consistent with the GATE results of LZ. They are consistent with those from four midtropospheric flights in Hurricanes Cleo, Daisy and Helene, 1958, reported by Gray (1965). MONEX updraft cores (at thresholds $w_i = 1 \text{ m s}^{-1}$) were of median width 1.4 km, median peak updraft 3.2 m s^{-1} , mean updraft 2.3 m s^{-1} and $\log_{10}(\text{mass transport in } \text{kg s}^{-1} \text{ m}^{-1} \text{ normal to the flight track})$ equal to 3.4 (Table 2). MONEX downdraft cores were of median width 1.3 km, peak downdraft 2.6 m s^{-1} , mean downdraft 1.9 m s^{-1} and $\log_{10}(\text{mass transport})$ equal to 3.2. Updraft cores were twice as numerous as downdraft cores.

The main difference between the MONEX and LZ results is in the widths of cores. LZ show relatively numerous cores of small widths. This may be due largely to restriction in the present work to cores of peak speed exceeding 2 m s^{-1} . Also, LZ generally treated measurements made on straight flight legs of length about 100 km, and subtracted out the leg mean vertical velocity. Here no such adjustment was made: it was ascertained that measured vertical air velocity w stayed near zero in clear air by comparing time series of w with airborne photography. Evidence accumulates that w in clear air over the tropical oceans remote from the surface and from clouds does stay near zero.

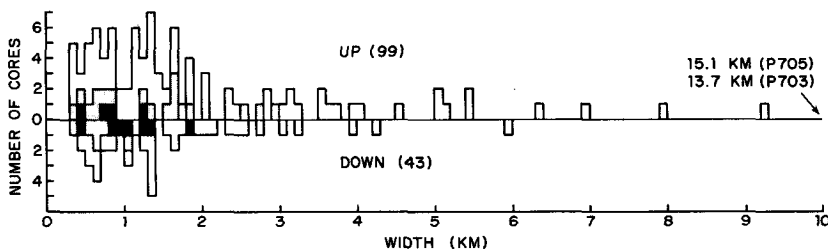


FIG. 4. Histograms of widths of convective cores of speed exceeding threshold $w_i = 1 \text{ m s}^{-1}$. Updrafts and downdrafts are respectively above and below the centerlines. Solid shading indicates draft cores in WMONEX, light shading those over the Arabian Sea (missions E620 and E624) and the remainder refer to the Bay of Bengal.

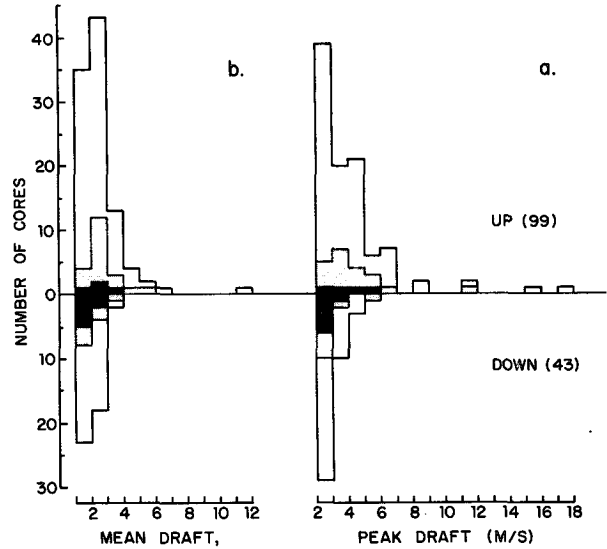


FIG. 5. Histograms of (a, right) peak drafts and (b, left) mean drafts, with updrafts extending above and downdrafts below the centerline. Results with $w_i = 1 \text{ m s}^{-1}$ are shown. Shading is as in Fig. 4.

6. Relationships between parameters of cores

Restating Eq. (5), the mass flux per meter normal to the aircraft track is the product of density, width and mean updraft:

$$F = \rho d \bar{w}, \tag{6}$$

$$\log_{10}(F) = \log_{10}(d) + \log_{10}(\bar{w}) + \log_{10}(\rho). \tag{7}$$

A good correlation was obtained by comparing $\log_{10}(F)$ with $\log_{10}(d)$; the points were stratified according to density (i.e. altitude); better correlations were obtained by comparing $\log_{10}(F)$ with $\log_{10}(\rho d)$: for all 134 updraft cores defined with $w_i = 2 \text{ m s}^{-1}$ the two correlation coefficients were respectively 0.953 and 0.979. The components shown in Eq. (7) are displayed in Fig. 7 for $w_i = 1 \text{ m s}^{-1}$ and Fig. 8 for $w_i = 2 \text{ m s}^{-1}$. In Figs. 7a and 8a, all ordinate values, and points along a central axis of symmetry of slope 45° , indicate $\log_{10}(F)$. Along the direction of the abscissa, to the left, the crosses (for updraft cores) and dots (for downdraft cores) show $\log(\rho d)$; the short lines show at one end, on the central

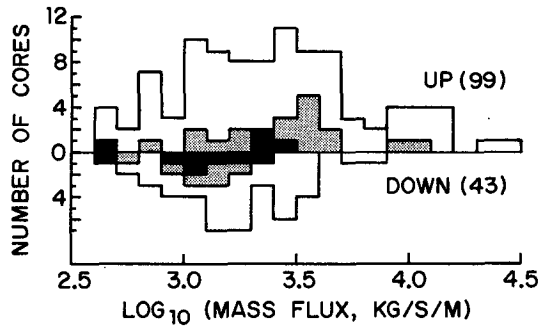


FIG. 6. Histograms of $\log_{10}(\text{mass flux})$ in the same format as in Fig. 4.

axis, $\log_{10}(F) = \log_{10}(\rho d \bar{w})$, and at the other end $\log_{10}(d \bar{w})$; the length of the short lines shows $\log_{10}(\rho)$. In most cases $\rho \approx 0.65 \text{ kg m}^{-3}$, so $\log_{10}(\rho) \sim -0.2$ and the short lines extend to the right of the 45° axis. Twelve draft cores (nine during mission E620, one during P707 and two during E714) were found in the boundary layer with $\rho \approx 1.1 \text{ kg m}^{-3}$, and the corresponding short lines extend to the left of the 45° axis. The displays of $\log_{10}(\rho)$ in Figs. 7a and 8a indicate no discernible trend of F with ρ or of ρd with ρ : draft cores at different altitudes had similar characteristics. Updraft cores (crosses) and downdraft cores (dots) had similar characteristics.

At the different thresholds w_i , points as in Fig. 8a representing $\log_{10}(F)$ versus $\log_{10}(\rho d)$ were constrained to values of $\log_{10}(F) > \log_{10}(\rho d w_i)$, because of Eq. (6): In Fig. 8a all the points lie above the line labeled $w_i = 2 \text{ m s}^{-1}$. At increasing values of F the points were

TABLE 2. Characteristics of cores from LeMone and Zipser (1980, LZ) for the middle troposphere and from this study with $w_i = 1 \text{ m s}^{-1}$. For the latter, missions are in parentheses and brackets indicate the same core.

	LZ	This study
Greatest width of updraft (km)	5.5	15.7 (P705)
Greatest upward mass flux [$\log_{10}(\text{kg s}^{-1} \text{ m}^{-1})$]	4.4	4.5 (P705)
Greatest peak updraft (m s^{-1})	17	17.4 (E714)
Greatest mean updraft (m s^{-1})	8	11.0 (E714)
Median width of updraft (km)	0.8	1.4
Median upward mass flux [$\log_{10}(\text{kg s}^{-1} \text{ m}^{-1})$]	~3.2	3.4
Median peak updraft (m s^{-1})	4.0	3.2
Median mean updraft (m s^{-1})	~2.5	2.3
Greatest width of downdraft (km)	2.2	5.9 (E718)
Greatest downward mass flux [$\log_{10}(\text{kg s}^{-1} \text{ m}^{-1})$]	4.0	3.9 (E718)
Greatest peak downdraft (m s^{-1})	7	5.1 (E620)
Greatest mean downdraft (m s^{-1})	4	3.1 (E620)
Median width of downdraft (km)	0.7	1.3
Median downward mass flux [$\log_{10}(\text{kg s}^{-1} \text{ m}^{-1})$]	~3.0	3.2
Median peak downdraft (m s^{-1})	2.4	2.6
Median mean downdraft (m s^{-1})	1.7	1.9

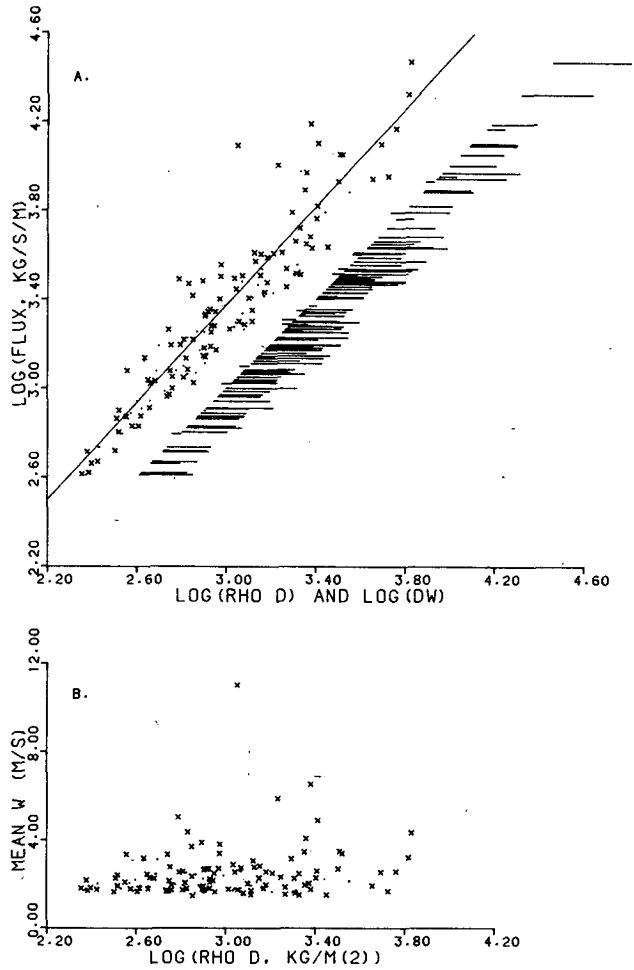


FIG. 7. (a, top): $\log_{10}(\text{mass flux}, F)$ on the ordinate plotted against $\log_{10}(\rho d)$ and $\log_{10}(d \bar{w})$ along the abscissa, for results with $w_i = 1 \text{ m s}^{-1}$. Points refer to (ρd) , with crosses for updraft cores and dots for downdraft cores. At the same level on the ordinate, short lines show at one end along a central 45° axis $\log_{10}(F = \rho d \bar{w})$, and at the other end $\log_{10}(d \bar{w})$. The lengths indicate the magnitude of $\log_{10}(\rho)$. A linear regression line is drawn through the crosses. (b, bottom): Mean draft core speed (\bar{w}) plotted against $\log_{10}(\rho d)$ with crosses for updraft cores and dots for downdraft cores.

increasingly distant from the corresponding w_i lines, and suggested linear relationships between $\log_{10}(F)$ and $\log_{10}(\rho d)$ of the form

$$\log_{10}(F) = b \log_{10}(\rho d) + \log_{10}(a). \quad (8)$$

Results of calculations of linear regression to obtain $\log_{10}(a)$ and b are given in Table 3. The appropriate regression lines, for updraft cores only, are drawn in Figs. 7a and 8a. From study of these plots, those for the other thresholds w_i (not shown here), and Table 3, bearing in mind the constraint that $\log_{10}[F] > \log_{10}[\rho d w_i]$, it appears that $b \approx 1.22$ is representative. For both updrafts and downdrafts with $w_i = 2 \text{ m s}^{-1}$, the following is quite a good approximation

$$F \approx 0.74(\rho d)^{1.22}. \quad (9)$$

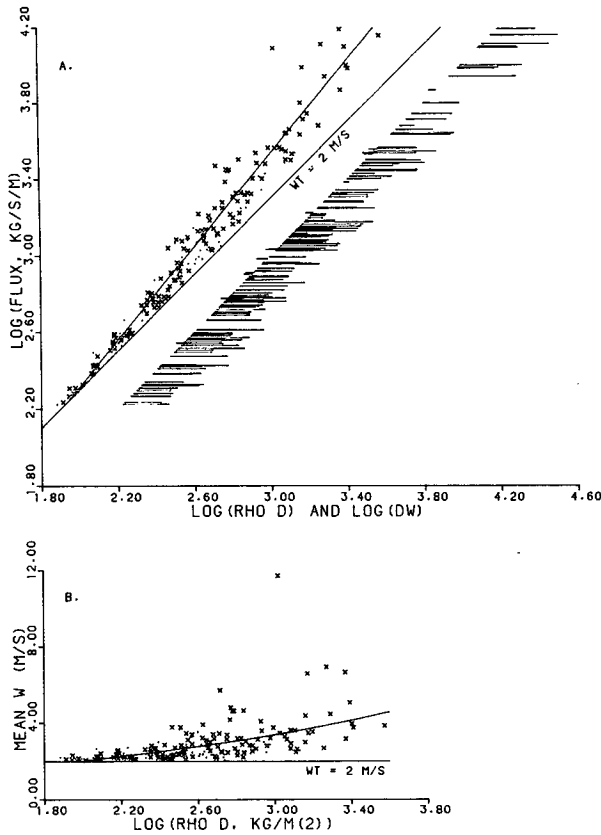


FIG. 8. As in Fig. 7, but for $w_t = 2 \text{ m s}^{-1}$. Lines representing the condition $w_t = 2 \text{ m s}^{-1}$ have been added. In (b), the curved line represents Eq. (10).

Denoting the mean vertical velocity at threshold w_t as $\bar{w}(w_t)$, combination of (9) and (6) yields

$$\bar{w}(2) \approx 0.74(\rho d)^{0.22}. \quad (10)$$

Plots of $\bar{w}(1)$ against ρd and $\bar{w}(2)$ against ρd are shown in Figs. 7b and 8b respectively. Most of the values of \bar{w} lie within quite narrow ranges. Eq. (10) is superimposed on Fig. 8b and represents most of the updraft and downdraft cores quite well. The outlying points of great mean w are not represented well. These

TABLE 3. Results from linear regression of $\log_{10}(F, \text{ kg s}^{-1} \text{ m}^{-1})$ against $\log_{10}(\rho d, \text{ kg m}^{-2})$.

Up or downdraft cores	w_t (m s ⁻¹)	Number of cores	Correlation coefficient	Parameters in Eq. (8)	
				b	a
Up	1	99	0.931	1.10	1.21
Down	1	43	0.965	0.95	2.72
Up	2	134	0.979	1.22	0.74
Down	2	49	0.983	1.06	1.68
Up	3	79	0.974	1.22	1.13
Up	4	52	0.982	1.25	1.20
Up	5	56	0.977	1.18	2.34

are cases of great peak w , of cumulonimbus cores (sometimes called “hot towers”) in the midtroposphere. An inventory of cores of peak $w \geq 8 \text{ m s}^{-1}$ is given in Table 5.

It is desirable to replace $\bar{w}(2)$ in (10) by $\bar{w}(0)$. To do this, relationships between peak vertical velocities and mean vertical velocities were studied. Results with $w_t = 1 \text{ m s}^{-1}$ are shown in Fig. 9. Results of linear regression analyses are given in Table 4, for the equation

$$w_p = p\bar{w} + q. \quad (11)$$

It is found that $1.68 < p < 1.87$ for both updraft and downdraft cores. To good approximation

$$w_p \approx 1.87\bar{w}(2) - 1.7. \quad (12)$$

For $w_t = 0$ it is necessary that $q = 0$. Consistency of slopes p of the graphs indicates that

$$w_p \approx 1.87\bar{w}(0). \quad (13)$$

Eliminating w_p between (12) and (13) and returning to (10), the following generalization is obtained

$$\bar{w}(0) \approx \pm[0.74(\rho d)^{0.22} - 0.9], \quad (14)$$

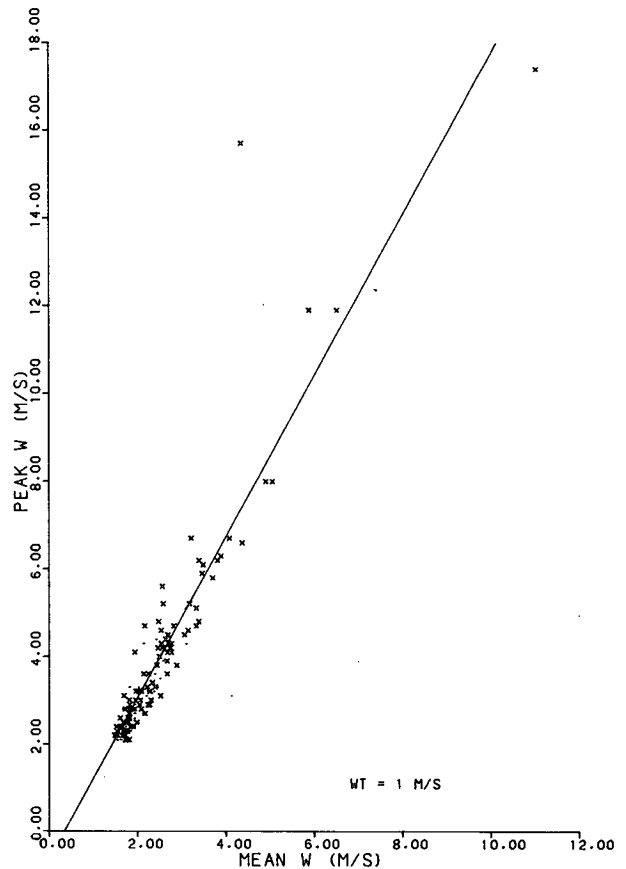


FIG. 9. Peak plotted against mean vertical speeds in draft cores for $w_t = 1 \text{ m s}^{-1}$. Crosses show updraft cores and dots downdraft cores. The linear regression line refers to the updraft cores only.

TABLE 4. Results from linear regression of peak against mean vertical velocities.

Up or downdraft cores	w_i (m s ⁻¹)	Number of cores	Correlation coefficient	Parameters in Eq. (11)	
				p	q
Up	1	99	0.918	1.84	-0.6
Down	1	43	0.879	1.68	-0.5
Up	2	134	0.965	1.87	-1.7
Down	2	49	0.964	1.77	-1.5
Up	3	79	0.984	1.71	-2.0
Up	4	52	0.984	1.71	-2.8
Up	5	56	0.984	1.78	-3.8

the \pm signs referring respectively to updraft and downdraft cores. We have measured, and subjectively examined, clouds recorded continuously by photography during most of the missions treated here. For ordinary tropical oceanic cumulus mediocris or congestus in the growing stage, it seems that (14) is likely to yield good estimates of mean updraft if d is taken as equal to the width of the cloud tower measured a few hundred meters below the top (Warner, 1981). A typical MONEX cumulus mediocris at altitude 2.5 km has $\rho \approx 0.9 \text{ kg m}^{-3}$ and $d \approx 1000 \text{ m}$, with the cloud top rising at $\sim 4 \text{ m s}^{-1}$. Eq. (14) yields $\bar{w} \approx 2.4 \text{ m s}^{-1}$. A typical MONEX cumulus congestus at altitude 6 km has $\rho \approx 0.64 \text{ kg m}^{-3}$ and $d \approx 1500 \text{ m}$, with the cloud top rising at $\sim 7 \text{ m s}^{-1}$. Eq. (14) yields $\bar{w} \approx 2.5 \text{ m s}^{-1}$. The cloud top rise rates quoted above are derived from airborne photogrammetry by noting height increments per unit time as a function of (slowly varying) measured cloud width. Values of \bar{w} equal to roughly half the cloud top rise rates are expected, so (14) appears to be a good approximation. However, it would underestimate the strongest draft cores in cumulonimbus clouds by a factor of 3 or more.

7. Summary

It has been found possible to obtain 2 s vertical air velocities to accuracy a few meters per second or better from standard measurements made aboard the NCAR Electra L-188 aircraft during MONEX when the gust probe system was not operative. An improved relationship was found between lift coefficient C_L for the Electra and angle of attack α (radians):

$$C_L = 0.347 + 6.37\alpha.$$

Characteristics were examined of 99 different updraft and 43 downdraft cores encountered during 16 MONEX research aircraft missions over the South China Sea, Arabian Sea and Bay of Bengal. These did not vary with geographical location; they were similar to those of draft cores over the tropical Atlantic described by LeMone and Zipser (1980). Draft cores were found either in cloud or close to the surface in the subcloud layer. Updraft cores were twice as numerous as downdraft cores. Updraft cores were often clustered in groups over distances up to 50 km, and not compensated locally by downdraft cores. On the other hand, traverses of $\sim 100 \text{ km}$ were often completed in anvil cloud without finding a single core exceeding 2 m s^{-1} .

Ignoring vertical air speeds less than the threshold 1 m s^{-1} , MONEX updraft cores were of median width 1.4 km, median peak updraft 3.2 m s^{-1} , mean updraft 2.3 m s^{-1} and $\log_{10}(\text{mass transport, in kg s}^{-1} \text{ m}^{-1} \text{ normal to the flight track})$ equal to 3.4. Downdraft cores were of median width 1.3 km, peak downdraft 2.6 m s^{-1} , mean downdraft 1.9 m s^{-1} and $\log_{10}(\text{mass transport})$ equal to 3.2.

For draft cores other than in vigorous cumulonimbus, the following equation was found relating mean draft speed \bar{w} (m s^{-1}), air density ρ (kg m^{-3}) and width d (m):

$$\bar{w} \approx \pm[0.74(\rho d)^{0.22} - 0.9],$$

TABLE 5. Tabulation of draft cores of peak vertical velocity $\geq 8 \text{ m s}^{-1}$.

Mission	Position of peak draft (°E, °N)	Pressure (hPa)	Time of peak draft (GMT)	w_i (m s ⁻¹)	Duration (s, m)	Peak draft (m s ⁻¹)	Mean draft (m s ⁻¹)	Mass flux (kg s ⁻¹ m ⁻¹)
P9	105.02, -1.55	445	228:44	5	1.4, 230	9.5	7.3	970
P9	105.02, -1.56	444	228:48	5	1.3, 220	9.3	7.2	920
P9	105.03, -1.75	444	231:16	5	6.8, 1010	8.9	7.4	4300
P10	113.18, 7.01	388	907:04	5	6.1, 960	17.3	11.7	5900
P10	113.06, 6.85	390	909:20	5	7.1, 1160	13.3	9.0	5500
P11	112.90, 6.54	390	957:29	5	10.2, 1560	10.1	7.4	6000
P17	112.82, 7.11	391	558:34	5	1.2, 210	13.3	9.2	1030
P17	112.65, 7.00	391	600:47	5	3.0, 440	12.2	9.0	2100
P17	112.63, 6.99	389	601:07	5	6.4, 970	9.9	7.0	3500
P17	112.62, 6.98	390	601:19	5	8.5, 1360	8.2	6.9	4900
E620	70.23, 16.41	479	853:10	1	20.1, 2750	11.9	5.9	10000
P705	89.93, 15.67	323	1006:28	1	88.8, 15150	15.7	4.4	29500
E708	87.52, 16.20	500	450:50	1	9.0, 1250	8.0	5.9	4800
E708	87.53, 16.16	493	451:25	1	27.7, 3790	11.9	6.5	15600
E714	89.09, 21.34	480	836:40	1	13.6, 1810	17.4	11.0	12400
E718	88.55, 20.73	529	731:48	1	7.0, 910	8.0	5.1	3100

the \pm signs referring to updraft and downdraft cores respectively. Generally $\bar{w} \approx 2.5 \text{ m s}^{-1}$.

Draft cores were similar to those found over the tropical Atlantic by LeMone and Zipser (1980). The greatest peak updrafts were $\sim 17 \text{ m s}^{-1}$, found on two occasions (identified in Table 5).

This study gives empirical results about individual convective cores. Theories of cumulus should yield results compatible with them. Isolated convective drafts over the tropical oceans reach only a few meters per second, except in cumulonimbi.

Acknowledgments. MONEX researchers are fortunate to be using the sophisticated research aircraft operated by NCAR and NOAA. We thank D. H. Lenschow, R. B. Friesen, R. L. Grossman and H. N. Zrubek of NCAR for generous help in these studies, and David P. Jorgensen and Herbert Riehl for helpful comments. This material is based upon work supported by the Division of Atmospheric Sciences, National Science Foundation, under Grants ATM-8012214 and ATM-8210128.

APPENDIX A

Calculations of Vertical Air Velocity from Measurements Aboard the Electra Aircraft

1. Theory

In LeMone and Zipser (1980) is given the equation for vertical air velocity w used here

$$w = V_z + U \cos\theta(\tan\alpha \cos R - |\tan\beta \sin R| - \tan\theta) + L \cos\theta(d\theta/dt), \quad (\text{A1})$$

where

- V_z aircraft vertical velocity (measured using INS)
- U true airspeed (pitot-static tube)
- θ pitch angle (INS)
- α attack angle (vanes)
- R roll angle (INS)
- β sideslip angle (vanes)
- L the longitudinal distance between the INS and the vanes
- t time.

The term INS refers to an inertial navigation system of measurement, and the term vanes to a gust probe. Lenschow *et al.* (1978) describe the measurements. Following Kelly and Lenschow (1978), let us consider MONEX research flights in which the Electra was flown straight and level, with vanes not operating, so that the last term in Eq. (A1) is dropped. For nominally straight and level flight let us take the sideslip term to be negligible. Then Eq. (A1) becomes

$$w = V_z + U \cos\theta \tan\alpha \cos R - U \sin\theta. \quad (\text{A2})$$

We have everything on the right-hand side except α .

The attack angle α is related to the lift coefficient C_L by a linear equation

$$C_L = C_{LO} + a\alpha, \quad (\text{A3})$$

where a and C_{LO} are constants. The coefficient C_L is given by

$$M(g + dV_z/dt) = 0.5C_L\rho AU^2, \quad (\text{A4})$$

where M is mass of the aircraft; g , gravitational acceleration; ρ , air density; and A , wing area.

The mass of the Electra is given to good approximation by a linear equation

$$M = M_0 - Ft, \quad (\text{A5})$$

where M_0 is the mass at take-off, F is the rate of fuel consumption, and t is the time measured from take-off. From pilots' logs of $M(t)$ —provided through R. B. Friesen—values of M_0 and F were found. Results are insensitive to fine tunings of M_0 and F . The wing area A is given by H. N. Zrubek (of the Research Aviation Facility, NCAR), as 121 m^2 .

It remains only to establish the constants in Eq. (A3), a and C_{LO} . From the manufacturers, Lockheed Corporation, R. L. Grossman has relayed the two pairs of values ($\alpha = -3.95^\circ$, $C_L = 0$) and ($\alpha = 10^\circ$, $C_L = 1.31$), yielding $a = 5.38$ per radian and $C_{LO} = 0.371$. These values are well outside the normal operating range $0^\circ < \alpha < 4.5^\circ$. A method described below has yielded $a = 6.37$ and $C_{LO} = 0.347$.

2. A relationship between C_L and α

For much of the time during MONEX, the Electra flew in clear air remote from clouds in the mid-troposphere over the tropical oceans. The vertical air motion mostly fluctuated around zero at tenths of meters per second or less. With $w = 0$, Eq. (A2) can yield α . With measurements of temperature and dew point to yield ρ , Eq. (A4) can yield C_L . On the magnetic tapes of stored data, all quantities measured aboard the Electra are 1 s average values prepared at NCAR under the direction of R. B. Friesen from analog signals recorded digitally at 50 Hz. The term dV_z/dt in Eq. (A4) was calculated as $V_{z_{n+1}} - V_{z_n}$, where n and $n + 1$ are one-second time steps; all the other quantities leading to α and to C_L were mean values, such as $0.5(U_n + U_{n+1})$. Calculated values of α and C_L were then plotted by computer on a scattergram, with expectations of a linear trend as in Eq. (A3). A MONEX research flight typically yielded 25000 data points, too many for one plot, so portions of flight were selected, early in the flight with relatively great values of M , α and C_L , near the middle, and late in the flight with relatively small values of M , α and C_L . To avoid circumstances involving significant vertical air velocity w , Electra side camera movies were used to choose portions of flight remote from clouds. Warner was

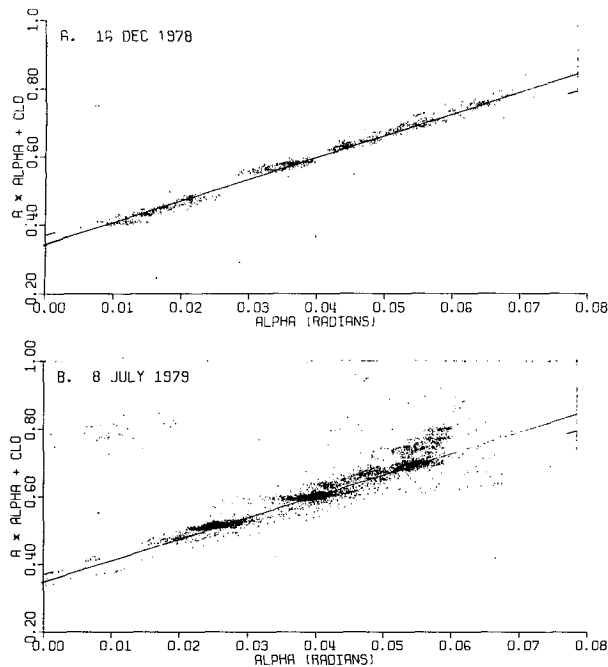


FIG. A1. Scattergrams of lift coefficient plotted on the ordinate against attack angle on the abscissa for selected intervals on (a) 16 December 1978 and (b) 8 July 1979. Calculated lift coefficients outside the range 0.2–1.0 were set to 1.0. Calculated attack angles > 0.0785 rad (4.5°) were set to 0.0785 rad. Tick marks indicate a straight-line relationship derived from the aircraft manufacturer. The straight lines drawn fully indicate Eq. (A6).

aboard the aircraft on both of two missions chosen for this study, that of 16 December 1978 over the South China Sea (WMONEX) and that of 8 July 1979 over the Bay of Bengal (SMONEX). The air was generally calm rather than bumpy. Computer plots of C_L versus α are shown for these two missions in Fig. A1.

Scattering of points occurs in Fig. A1, but a linear trend of C_L with α emerges very nicely. Parts a and b of Fig. A1 were superimposed and the following equation found by eye

$$C_L = 0.347 + 6.37\alpha. \quad (\text{A6})$$

This line is drawn in Fig. A1. It fits much better than the manufacturer's relationship, indicated by line elements just inside the edges of the figure. The rela-

tionship from Lockheed probably came from an Electra fitted as an airliner rather than a laboratory.

In getting Eq. (A6), emphasis was placed on the points at very small α , and the groups of points near $\alpha \approx 0.053$ rad. Drawn thus, the heavy clusters also are fit well. Why is there scatter in the figures? Partly because of very light turbulence, with 1 s values of w reaching $\sim 1 \text{ m s}^{-1}$. Points to the right of the line correspond to $w > 0$, those to the left to $w < 0$. The group of anomalous points near $\alpha = 0.06$ rad in Fig. A1b came from occasions on which $0.5 < V_z < 1 \text{ m s}^{-1}$. Regular features of Electra flights during MONEX were oscillations induced by an autopilot, involving heading and roll, so some scatter is expected.

Satisfied with Eq. (A6), one may use (A5) to get M , then (A4) to get C_L , then (A6) to get α , and finally (A2) to get values of w , as a series of values every second, each involving averaging over ~ 2 s.

REFERENCES

- Fein, J. S., and J. P. Kuettner, 1980: Report on the Summer MONEX field phase. *Bull. Amer. Meteor. Soc.*, **61**, 461–474.
- Gray, W. M., 1965: Calculations of cumulus vertical draft velocities in hurricanes from aircraft observations. *J. Appl. Meteor.*, **4**, 463–474.
- Greenfield, R. S., and T. N. Krishnamurti, 1979: The Winter Monsoon Experiment—Report of December 1978 field phase. *Bull. Amer. Meteor. Soc.*, **60**, 439–444.
- Kelly, T. J., and D. H. Lenschow, 1978: Thunderstorm updraft velocity measurements from aircraft. *Preprints, 4th Symp. on Meteor. Observations and Instrumentation*, Denver, Amer. Meteor. Soc., 474–478.
- LeMone, M. A., and W. T. Pennell, 1980: A comparison of turbulence measurements from aircraft. *J. Appl. Meteor.*, **19**, 1420–1437.
- , and E. J. Zipser, 1980: Cumulonimbus vertical velocity events in GATE. Part I: Diameter, intensity and mass flux. *J. Atmos. Sci.*, **37**, 2444–2457.
- Lenschow, D. H., C. A. Cullian, R. B. Friesen and E. N. Brown, 1978: The status of air motion measurements on NCAR aircraft. *Preprints, 4th Symp. on Meteor. Observations and Instrumentation*, Denver, Amer. Meteor. Soc., 433–438.
- Merceret, F. J., and H. W. Davis, 1981: The determination of navigational and meteorological variables measured by NOAA/RFC WP-3D aircraft. NOAA Tech. Memo. ERL RFC-7, 21 pp. Research Facilities Center, Miami, FL.
- Warner, C., 1981: Photogrammetry from aircraft side camera movies: Winter MONEX. *J. Appl. Meteor.*, **20**, 1516–1526.
- Zipser, E. J., and M. A. LeMone, 1980: Cumulonimbus vertical velocity events in GATE. Part II: Synthesis and model core structure. *J. Atmos. Sci.*, **37**, 2458–2469.
- , R. J. Meitin and M. A. LeMone, 1981: Mesoscale motion fields associated with a slowly moving GATE convective band. *J. Atmos. Sci.*, **38**, 1725–1750.